Systemic RALA/iNOS nanoparticles; a potent gene therapy for metastatic breast cancer coupled as a biomarker of treatment

Accepted Manuscript

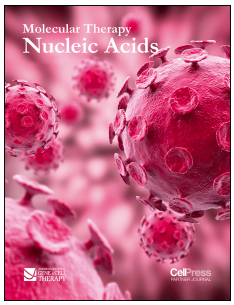

Systemic RALA/iNOS nanoparticles; a potent gene therapy for metastatic breast cancer coupled as a biomarker of treatment

Cian M. McCrudden, John W. McBride, Joanne McCaffrey, Ahlam A. Ali, Nicholas J. Dunne, Vicky L. Kett, Jonathan A. Coulter, Tracy Robson, Helen O. McCarthy

PII: S2162-2531(16)30378-X

DOI: 10.1016/j.omtn.2016.12.010

Reference: OMTN 21

To appear in: *Molecular Therapy: Nucleic Acid*

Received Date: 30 November 2016

Revised Date: 8 December 2016

Accepted Date: 8 December 2016

Please cite this article as: McCrudden CM, McBride JW, McCaffrey J, Ali AA, Dunne NJ, Kett VL, Coulter JA, Robson T, McCarthy HO, Systemic RALA/iNOS nanoparticles; a potent gene therapy for metastatic breast cancer coupled as a biomarker of treatment, *Molecular Therapy: Nucleic Acid* (2017), doi: 10.1016/j.omtn.2016.12.010.

Systemic RALA/iNOS nanoparticles; a potent gene therapy for metastatic breast cancer coupled as a biomarker of treatment

Cian M. McCrudden[1], John W. McBride[1], Joanne McCaffrey[2], Ahlam A. Ali[1], Nicholas J. Dunne[3], Vicky L. Kett[1], Jonathan A. Coulter[1], Tracy Robson[4], Helen O. McCarthy[1,*]

[1]School of Pharmacy, Queen's University Belfast, 97 Lisburn Road, Belfast, Northern Ireland, BT9 7BL

[2] Dept. of Pharmacology & Therapeutics, University College Cork, Cork, Ireland

[3] School of Mechanical and Manufacturing Engineering, Dublin City University, Dublin, Ireland

[4] Royal College of Surgeons in Ireland, 123 St Stephen's Green, Dublin 2, Ireland.

Correspondence should be addressed to H.O.M. (h.mccarthy@qub.ac.uk)

Dr Helen McCarthy, Experimental Therapeutics, School of Pharmacy, Queen's University Belfast, Belfast BT9 7BL. h.mccarthy@qub.ac.uk Tel: +442890972149, Fax: +442890247794

Work was carried out in Belfast, United Kingdom

Short title – iNOS gene therapy in metastatic breast cancer

Abstract

This study aimed to determine the therapeutic benefit of a nanoparticular formulation for the delivery of inducible nitric oxide synthase (iNOS) gene therapy in a model of breast cancer metastasis. Nanoparticles comprising a cationic peptide vector, RALA, and plasmid DNA were formulated and characterized using a range of physiochemical analyses. Nanoparticles complexed using iNOS plasmids and RALA approximated 60 nm in diameter, with a charge of 25 mV. A vector neutralization assay, performed to determine the immunogenicity of nanoparticles in immunocompetent C57BL/6 mice, revealed that no vector neutralization was evident. Nanoparticles harboring iNOS plasmids (constitutively active cytomegalovirus (CMV)-driven, or transcriptionally-regulated human osteocalcin (hOC)-driven) evoked iNOS protein expression and nitrite accumulation, and impaired clonogenicity in the highly aggressive MDA-MB-231 human breast cancer model. Micrometastases of MDA-MB-231-luc-D3H1 were established in female BALB/c SCID mice by intracardiac delivery. Nanoparticulate RALA/CMV-iNOS or RALA/hOC-iNOS increased mean survival in mice bearing micrometastases by 27% compared to controls, and also provoked elevated blood nitrite levels. Additionally iNOS gene therapy sensitized MDA-MB-231-luc-D3H1 tumors to docetaxel treatment. Studies demonstrated that systemically delivered RALA-iNOS nanoparticles has therapeutic potential for the treatment of metastatic breast cancer. Furthermore, detection of nitrite levels in the blood serves as a reliable biomarker of treatment.

Introduction

An obstacle to genetic therapies is the absence of a vector with the DNA-delivery ability of a virus that lacks the immunogenicity commonly associated with viral vectors. We have developed a cationic fusogenic peptide vector, RALA, that on exposure to anionic nucleic acids, self assembles into nanoscale particles suitable for cell membrane penetration. Endosomal escape, consequent of conformational change at low pH ensures that the genetic cargo can reach the nucleus and achieve transgene expression. [1] We previously demonstrated the remedial potential of RALA-delivered therapeutic cargoes; growth of ZR-75-1 breast cancer xenografts was abrogated by plasmid FK506-binding protein-like (FKBPL), [2] while nanocomplexation of anionic bisphosphonates with RALA afforded the agents cytotoxicity against PC-3 prostate cancer cells *in vitro* and in xenografts following intratumoral injection. [3] In this study, we aimed to provoke a therapeutic benefit in a model of aggressive breast cancer by nanocomplexation of plasmid inducible nitric oxide synthase (iNOS) with RALA.

The paradoxical relationship between nitric oxide (·NO) and transformed tissue, whereby low concentrations of the gasotransmitter provoke an aggressive phenotype, but higher concentrations are detrimental to the tumor, [4] has led to a divergence in the discipline, with attempts being made to either promote or interfere with ·NO signaling. The mechanisms by which ·NO mediates its effects in neoplastic conditions are diverse, but can be broadly characterized into promotion (low ·NO) or inhibition (high ·NO) of apoptosis, promotion (low) or inhibition (high) of proliferation, and stimulation (low) or

attenuation (high) of angiogenesis.[4] ·NO can react with inorganic molecules (i.e. oxygen, superoxide or transition metals), structures in DNA, prosthetic groups or proteins, and can elicit beneficial or detrimental responses dependent on radical concentration and local environmental conditions.[5] Host macrophages that infiltrate tumors rely partially on the cytotoxic properties of ·NO to evoke an anti-tumoral response.[6]

The majority of attempts to exploit the tumoricidal properties of ·NO involve using a ·NO donor molecule. Many such donors exist, and are broadly represented by the organic nitrates, metal-NO complexes, *S*-nitrosothiols, sydnonimines, diazeniumdiolates (NONOates), and ·NO-drug hybrids.[4] One ·NO-donating prodrug that has received particular attention is JS-K; JS-K induced apoptosis in a range of breast cancer cell lines, but spared normal HMEC endothelial cells and MCF-10A.[7] JS-K was recruited onto the National Cancer Institute's Rapid Access to Interventional Development (RAID) program, accelerating its progression as a potential therapeutic.[8]

As an alternative approach to achieving therapeutic levels of intra-tumoral ·NO, we[9-14], and others[15-17] have demonstrated the benefit of iNOS as a therapeutic transgene. Constitutive iNOS expression abolished clonogenicity in ZR-75-1 breast cancer cells,[13] and sensitized to cisplatin in human cancer cell lines and murine RIF-1 xenografts,[9] and in A549 models of human primary and metastatic lung cancer.[17] To limit ·NO release from an iNOS gene therapeutic to target tumors, we have deployed a transcriptional targeting approach using the human osteocalcin (hOC) promoter to drive iNOS expression. The hOC promoter is activated by transcription factors such as Runx2 and

Fra-2, which are commonly overexpressed in cancers that metastasise to bone.[18] hOC-iNOS-derived ·NO achieved almost complete elimination of colony forming ability in PC-3 and DU145 castration-resistant prostate cancer cells, as well as inducing stasis in PC-3 xenografts.[11,19]

The purpose of the current study was to determine whether cationic RALA-based nanoparticles carrying an iNOS transgene had a therapeutic impact in mice bearing MDA-MB-231 (known to be sensitive to ·NO donor DETA/NO, through generation of dinitrogen trioxide[20]) micrometastases.

Results

Nanoparticle characterization

Incubation of RALA with plasmid DNA in water resulted in the formation of nanoparticles with physical characteristics suitable for cellular internalization (**Figure 1a**)[1,2,21].

Subcellular nanoparticle localization

Labeling with Cy3 did not impact the physicochemical properties of nanoparticles (**Figure 1b**). The ability of RALA to deliver Cy3-labeled pEGFP-1 nanoparticles to the nucleus of MDA-MB-231-luc-D3H1 was confirmed by confocal fluorescence microscopy using orthogonal sectioning (to construct XZ and YZ images to correspond to an area of interest in an XY image following collection of a Z-stack of images); by 60 min following commencement of transfection, Cy3 fluorescence was evident within the confines of the cell, and within 120 min, was detected within the nucleus (**Figure 1c**).

Vector neutralization assay

The transfecting potency of RALA/pEGFP-N1 in ZR-75-1 breast cancer cells was not detrimentally affected by incubation of the nanoparticles with pooled sera from mice that had received RALA/pEGFP-N1 nanoparticles (single or multiple administrations thereof). Repeated measures two-way ANOVA with Dunnett's correction for multiple comparisons was used to compare sera from nanoparticle-treated mice with other treatments (**Figure 2a**). In no case did incubation in sera from nanoparticle-treated mice lessen GFP expression; rather, nanoparticles incubated in sera from nanoparticle-treated mice provoked slightly higher transfection ability. The degree of fluorescence of ZR-75-1 was diminished slightly when nanoparticles were incubated in 10% serum, although this cannot be down to antibody neutralization, as nanoparticles incubated in sera from mice that received PBS, pDNA or RALA only, or those incubated in FBS also evoked less fluorescence when serum concentration was 10% (**Figure 2b**).

Sera from mice that received PBS, pEGFP-N1, RALA or RALA/pEGFP-N1 nanoparticles produced limited immunoreactivity in RALA/pEGFP-N1 nanoparticle-coated wells of an ELISA plate (**Figure 2c**). There was no significant difference ($P>0.05$) in immunoreactivity between sera from mice that received nanoparticles and mice that received any other treatment (repeated measures two-way ANOVA with Tukey multiple comparisons test).

iNOS transgene expression in MDA-MB-231-luc-D3H1

Transfection of MDA-MB-231-luc-D3H1 with CMV- or hOC-iNOS provoked accumulation of nitrites in culture medium as analyzed 48 h post transfection; iNOS protein expression was also detectable by western blot (**Figure 3a**).

Clonogenics

MDA-MB-231-luc-D3H1 transfected with RALA/hOC-iNOS (61.70% ± 10.39) or RALA/CMV-iNOS (68.40% ± 13.32) had lower clonogenicity than untransfected control cells. Treatment with 1 mM aminoguanidine (NOS inhibitor) [22] partially blocked this inhibition of clonogenicity, (79.4% ± 16.2 and 85.4% ± 15.6 of control for RALA/hOC-iNOS and RALA/CMV-iNOS respectively) (**Figure 3b**). Optimization of transfection conditions are summarized in **Supplemental Figure S1**.

RALA/iNOS gene therapy slows progression of metastatic breast cancer in mice

Administration of hOC/CMV-iNOS-loaded RALA nanoparticles delayed bioluminescence accumulation (**Figure 4a, 4d**) and disease progression in mice bearing MDA-MB-231-luc-D3H1 micrometastases (**Figure 4b**). Control and vehicle only mice had a median post-implantation survival of 31.5 and 30.0 days respectively. Median survival was significantly increased (Log-rank (Mantel-Cox) test) by treatment with RALA/hOC-iNOS (38.5 days; $P = 0.001$), and RALA/CMV-iNOS therapy (40 days; $P > 0.001$).

Figure 4c and 4d comprises biochemical and physical data from a single mouse per treatment group (those individuals whose post-implantation survival was closest to the

relevant treatment's median value – cumulative data of all mice are presented in **Supplemental Figures S2 and S3**). Mice that received iNOS transgenes lost mass (Figure 4c) and developed bioluminescent signal (**Figure 4d**) more slowly than control.

Blood nitrite levels in both RALA/iNOS complex-receiving mice were up to nine-fold higher than the blood nitrite levels of control mice (Figure 4e). Opsonization and sequestration by the mononuclear phagocyte system is a common fate of cationic nanoparticles following systemic administration – this could explain why gene expression following treatment with RALA/pLuciferase [1] and other similarly charged gene therapy nanoparticles [23] is seen mainly in the lungs and liver of mice. To determine whether these organs were less susceptible to metastases colonization in RALA/iNOS-treated mice, we attempted to quantify the number of metastatic lesions in mice at endpoint, and to make an estimation of the location of the lesions. The number of lesions evident in the final images (i.e. experimental endpoint) of each mouse was counted, their location was assigned to one of head, thoracic, abdominal or skeletal, and the number at each location was counted. Mice that received iNOS gene therapy had fewer metastatic foci than control mice, and RALA/CMV-iNOS or RALA/hOC-iNOS treatment appeared to inhibit metastases development in the abdominal cavity and the head, but had no impact on lesion development in the skeleton or thoracic cavity (Supplemental Figure 4). The inhibition of lesion development in the abdomen may be due to iNOS gene overexpression in the liver, although we did not investigate this further.

iNOS sensitizes to docetaxel *in vitro* and *in vivo*

Transfection of MDA-MB-231-luc-D3H1 with either RALA/CMV-iNOS or RALA/hOC-iNOS nanoparticle complexes before treatment with docetaxel enhanced the docetaxel response. Docetaxel dose-dependently inhibited the viability of MDA-MB-231-luc-D3H1 (EC_{50} of 82.7 nM), while transfection with RALA/hOC-iNOS or RALA/CMV-iNOS reduced the EC_{50} to 33.3 nM and 34.9 nM respectively (both $p<0.05$, assessed by repeated measures one-way ANOVA with Geisser-Greenhouse correction; **Figure 5a**).

Metastases-bearing mice that were treated with docetaxel had a median survival of 44.0 days. Although co-administration of docetaxel with RALA/hOC-iNOS (46.0 days; P = 0.8601) or RALA/CMV-iNOS (49 days; P = 0.3757) complexes did not significantly improve median survival, maximal survival (51 days in docetaxel only) was considerably longer in both docetaxel + RALA/hOC-iNOS and RALA/CMV-iNOS treatment groups (78 and 86 days respectively; **Figure 5b**). **Figure 5c and 5d** represent mass loss and bioluminescence accumulation in individual mice whose survival was closest to median survival; cumulative data on all mice is presented in **Supplemental Figure S5**. As is evident in **Figure 5d**, luminescence accumulation was retarded in the gene therapy plus docetaxel groups until therapy was withdrawn, while in docetaxel-treated mice, luminescence accumulation progressed from day 5 onwards, although at a slower rate than in control.

Discussion

The evidence presented here demonstrates for the first time the therapeutic utility of iNOS gene therapy following systemic administration. In our assays, both RALA/iNOS strategies impressively prolonged the survival of mice bearing MDA-MB-231 micrometastases. Using blood nitrite measurements, we demonstrated that receiving either gene therapy regimen provoked ·NO generation in these mice. Assessment of circulating nitrite concentrations in this system was a viable biomarker for successful transgene expression; changes in ·NO flux have been used previously to confirm therapeutic ·NO generation [24], although this was by invasive insertion of an amiNO 700 probe.

Nanoparticles formed of RALA and either iNOS plasmid displayed size and charge characteristics suitable for cellular internalization. Indeed, our observations were in agreement with previous studies on the internalization of RALA/plasmid DNA nanoparticles, which occurs rapidly, and relies on both clathirin- and caveolin-dependent processes. [1] We have previously demonstrated that iNOS gene therapies delivered intratumorally produce an impressive therapeutic benefit [9-12,19], and described reporter gene expression when the luciferase gene was delivered systemically using RALA [1], but this is the first description of systemic RALA-mediated therapeutic transgene delivery, and the first description of systemically-delivered iNOS for cancer gene therapy. Both iNOS gene therapy constructs provoked inhibition of clonogenicity *in vitro*. ·NO exerts its anti-cancer benefit when its intracellular concentration is in the micromolar range [25]; although we did not assess intracellular ·NO concentration following transfection, the accumulation of nitrites in culture medium is indicative of considerable increase in intracellular ·NO content. The fate of transfected cells likely depends on the degree of

·NO production, but could include apoptosis, attraction of macrophages, or toxicity due to a bystander effect.[26]

A concern associated with indiscriminate production of ·NO is the deleterious side effects that may manifest, such as hypotension. Numerous strategies have been employed to limit ·NO production to the disease site, including β-galactosidase-provoked release of ·NO/HNO from IPA/NO,[27] or the nitroreductase-dependent release of ·NO from 1-(2-methylpiperidin-1-yl)diazen-1-ium-1,2-diolate.[28] Likewise, RRx-001, which preferentially releases ·NO in the hypoxic environment, attenuated murine SCC VII xenograft growth and sensitized to fractionated radiotherapy, doubling the survival time of mice.[29] Ligand targeting of nanoparticles is a common targeting strategy, with tumor-associated dysregulated expression of the receptors of transferrin, folic acid, epidermal growth factor and hyaluronic acid being particularly popular.[30] We have previously employed numerous transcriptional targeting strategies. Utilization of the prostate specific membrane antigen (PSMA) promoter elicited iNOS transgene expression in prostate cancer lines, but not in colon or breast carcinoma lines.[11] We have also used inducible promoters to control iNOS expression; the WAF1/p21 promoter, whose activity is induced by radiation, when used to drive iNOS expression, evoked RIF-1 and HT29 tumor growth delay that exceeded that observed with either a fractionated radiotherapy strategy alone[12] or with a single X-ray dose (10 or 20 Gy).[14]

It was unsurprising that RALA/CMV-iNOS was more potent than RALA/hOC-iNOS, given the constitutive activity of the promoter, although the transcriptionally-targeted

therapy also significantly improved the survival of mice bearing metastases. Overexpression of Runx2, characteristic in MDA-MB-231 [31], is responsible for activation of the hOC promoter [18]. We have shown previously that PC3 prostate cancer cells express GFP and iNOS transgenes as provoked using hOC, but LNCaP prostate cancer cells do not [19]; LNCaP are known to express Runx2 to a much lower extent than PC3 [32]. Given that Runx2 expression is elevated in metastatic bone lesions of breast cancer patients, but absent in corresponding primary tumors [31], employment of a Runx2-activatable therapy should result in maximal iNOS transgene expression in the most aggressive tumor sites, and spare normal tissue [33]. Runx2 has also been implicated in the progression of prostate [34], lung [35] and thyroid [36] cancers, which preferentially target the bone for metastatic colonization. We expect that these and other tumors that overexpress Runx2 would benefit from hOC-iNOS gene therapy.

Despite the compelling evidence of therapeutic potential of iNOS gene therapy in neoplastic conditions [9,12,14-16,19,37,38], the dichotomy of the relationship between ·NO and the tumor environment confers skepticism when it comes to overexpressing ·NO. Although iNOS expression was negatively correlated with lesion grade in a cohort of invasive ductal breast carcinomas [39], indicating a possible role of iNOS in the prevention of metastasis, iNOS expression has conversely been implicated as a marker of poor prognosis in several malignancies, including prostate, colon and breast [40]. Stratification of a breast cancer patient cohort by estrogen receptor (ER) expression revealed that iNOS expression was predictive of poorer survival in ER^- patients [41], while high iNOS expression was similarly detrimental in a range of triple-negative breast cancer patient

cohorts. [42] Consequently, efforts are being made to repress iNOS activity as a therapeutic strategy - NOS inhibitors such as AG [22] have been investigated in pre-clinical settings, and more recently, ASP9853, an inhibitor of iNOS dimerization, was tested in combination with docetaxel in patients with advanced solid tumors [43].

However, while iNOS expression may correlate with disease status in some analyses, it is important to note that protein levels do not necessarily correlate with activity. Several factors could affect the translation of iNOS mRNA to functional protein, and the production of ·NO. In the mouse RENCA renal cancer cell line, iNOS mRNA expression is not translated into functional protein, resultant of post-transcriptional modification by miR-146a. Treatment of RENCA cells with anti-miR-146a restores the cells' ability to translate iNOS protein, with concurrent ·NO production, and xenografts of these cells had considerably slower growth dynamics than negative control anti-miR-treated cells. [44] miR-146a expression may impact iNOS expression in the clinical setting, potentially complicating prognostication based upon iNOS mRNA expression profiling. Indeed, miR-146a was overexpressed in triple-negative breast cancer cell lines (including MDA-MB-231), and was significantly overexpressed in triple-negative breast cancer patient samples than in non-triple-negative patients [45]. Another factor that plays a role in iNOS activity is its co-factor tetrahydrobiopterin; NOS enzymes in cancer cells may preferentially produce superoxide and peroxynitrite over ·NO itself, resultant of inappropriate tetrahydrobiopterin:dihydrobiopterin (BH4:BH2) proportions. Restoration of appropriate BH4:BH2 proportions in MCF-7 and MDA-MB-231 breast cancer cells using sepiapterin manifested dose-dependent cytotoxicity that was diminished when NOS

was inhibited. Oral sepiapterin also delayed MDA-MB-231 xenograft progression. In this model, aberrant BH4:BH2 proportion is likely to deprive the tumor of the therapeutic benefit afforded by ·NO [46].

We investigated the impact of iNOS overexpression on sensitivity to docetaxel. A taxane, docetaxel acts by preventing microtubule depolymerization, inhibiting mitosis. We did not determine whether the additive effect that we observed was down to sensitization to docetaxel, or the additive impact of iNOS overexpression and docetaxel treatment; MDA-MB-231s treated with 100 nM docetaxel arrested in G2/M phase of the cell cycle [47], while treatment with ·NO donor DETA-NONOate arrested MDA-MB-231s in G1 [48]. There is precedent for ·NO sensitizing to chemotherapy. In MDA-MB-231, hypoxia-induced resistance to doxorubicin and 5-HT was attenuated by treatment with nitroglycerin (a ·NO donor); low oxygen levels in conditions of hypoxia prohibit the biogenesis of ·NO, so these findings support a role for endogenous ·NO in chemosensitzation [49]. CMV-iNOS treatment sensitized human cancer cells to cisplatin *in vitro*, and also RIF-1 murine xenografts to the same *in vivo* [9]. In a C6 glioma model, overexpression of dimethylarginine dimethylaminohydrolase (DDAH) (which metabolizes asymmetric dimethylarginine (ADMA), an endogenous NOS inhibitor) sensitized C6 xenografts to docetaxel [50]. Additionally, in lung adenocarcinoma patients, nitroglycerin patch treatment improved response to docetaxel/carboplatin therapy [51]. It is likely that there is potential for RALA/iNOS therapy to similarly sensitize to docetaxel, and that optimization of the regimen is required to determine the best therapeutic window *in vivo*. It is also possible that iNOS gene therapy may be of more benefit in a model of

docetaxel resistance, which is more representative of those that have failed chemotherapy.

Conclusions

Our data demonstrate a clear anti-cancer effect of RALA/iNOS gene therapy for metastatic breast cancer. Overexpression of iNOS with concomitant increase in ·NO liberation is a strategy for direct cytotoxicity, and requires additional interrogation for its ability to sensitize to other cytotoxic approaches. Measurement of circulating nitrites was a method for confirmation of iNOS transgene activity, and could harnessed to determine iNOS therapeutic efficacy. The nucleic acid delivery ability of RALA is unquestionable; beyond utility as a reporter gene delivery vehicle [1], it effectively delivers siRNAs [2], and RALA/DNA nanoparticles were evaluated as components of a DNA vaccination device [21]. However, this is the first report validating systemically-delivered RALA/nucleic acid therapeutics. Further development of this potent RALA/iNOS treatment is required with respect to dosing, adjuvant therapies and increasing circulation times.

Materials and methods

Materials

Unless otherwise stated, reagents used were from Sigma (Dorset, UK).

Cell culture

ZR-75-1 breast cancer cells were purchased from ATCC, and maintained in RPMI-1640 (Life Technologies) supplemented with 10% fetal bovine serum (PAA). MDA-MB-231-luc-D3H1 were purchased from PerkinElmer Inc. (Buckinghamshire, UK) and maintained in DMEM (Life Technologies) supplemented with 10% fetal bovine serum (PAA). Cells were cultivated in 175 cm^2 flasks in a humidified incubator; once 80-90% confluency was reached, cells were passed to maintain exponential growth. Mycoplasma absence was confirmed monthly, using Plasmotest (Invivogen, France).

Plasmid DNA preparation

MAX Efficiency® DH5α™ Competent Cells containing relevant plasmids (pEGFP-N1/CMV-iNOS/hOC-iNOS) were cultured in a shaking incubator overnight at 37°C in Luria broth containing the appropriate antibiotic. Plasmid DNA was isolated and purified using PureLink® HiPure Plasmid Maxiprep Kits (Life Technologies, Paisley, UK), using the manufacturer's protocol. Plasmid DNA was dissolved in ultrapure water, and stored at -20°C.

Nanoparticle complexation and characterization

RALA was custom synthesized using solid-state synthesis (FMOC) (Biomatik, USA) and supplied as a desalted lyophilized powder. Reconstitution was in ultrapure water to a stock concentration of 5.8 mg/ml. Aliquots were stored at -20°C until use.

Plasmid DNA/RALA nanocomplexes were constructed as previously described [1]. Briefly, plasmid DNA was incubated with RALA for 30 min at room temperature to

facilitate electrostatic interaction of the anionic DNA with the cationic peptide. Nanoparticles were complexed at N:P10 (N:P ratio is the molar ratio of positively charged nitrogen atoms in the peptide to negatively charged phosphates in the pDNA backbone – at N:P10, 14.5 μg of RALA is used to neutralize 1 μg of DNA). Nanoparticles were analyzed in terms of their hydrodynamic size and particle charge using a Nano ZS Zetasizer and DTS software (Malvern Instruments, UK).

Intracellular nanoparticle tracking

Plasmid DNA (pEGFP-1 – analogous to pEGFP-N1, but lacking the promoter) was labeled with Cy3 using a Mirus Bio LabelIt® kit (Cambridge Bioscience, Cambridge, UK) as recommended by the manufacturer. Cy3-labeled DNA was complexed with RALA as before, and the impact of the fluorophore on nanoparticle size and charge was determined as above.

MDA-MB-231-luc-D3H1 were seeded in 24 well plates on round coverslips at 10^4 cells per coverslip, and allowed to adhere for 2 h; the wells were then supplemented with complete growth medium, and incubated overnight. Following 2 h starvation in Opti-MEM (Life Technologies), nanoparticle complexes were added to the Opti-MEM, and cells were transfected for 30, 60 and 120 min. Cell actin cytoskeleton was stained using FITC-conjugated phalloidin (Life Technologies), and coverslips were mounted onto microscope slides using Diamond Antifade with DAPI (Life Technologies).

Nanoparticle subcellular localization was analyzed in MDA-MB-231-luc-D3H1 by confocal fluorescence microscopy using a Leica SP5 microscope and LAS-AF software.

Clonogenic assay

The impact of RALA/iNOS on clonogenicity of MDA-MB-231-luc-D3H1 was assessed. MDA-MB-231-luc-D3H1 were seeded in T25 culture flasks at a density of 10^6 cells per flask, and incubated overnight. Following a 2 h starvation in Opti-MEM, cells were transfected with RALA/CMV-iNOS or RALA/hOC-iNOS nanoparticle formulations, equivalent to 6 μg DNA per flask; transfection was for 6 h, following which, transfection media were replaced with normal growth medium, and cells returned to the incubator for overnight incubation. Following 24 h, cells were trypsinized, counted and plated in triplicate in 6 well plates at 500/1000 cells per well. Plates were incubated at 37°C for 12 days, following which, colonies were fixed and stained using 0.4% crystal violet (Sigma) in 70% methanol; excess stain was removed by gentle washing in water, and once dry, colonies were manually counted. Treatment with 1 mM aminoguanidine (NOS inhibitor), where appropriate, began 24 h post plating into clonogenic plates.

Vector neutralization assay

Before commencing *in vivo* therapeutic assessment of RALA/iNOS nanoparticles, we determined whether repeated administration of nanoparticles induced vector neutralization in a competent immune system. Nanoparticles (comprising 10 μg pEGFP-N1 complexed with RALA at N:P10) were formulated as above in a volume of 100 μl. Treatments were delivered via the tail vein of male C57BL/6 mice (6-8 weeks old at

beginning of experiment) using a 29G insulin syringe (Terumo). PBS, and DNA and RALA only treatments were also performed. Treatments were administered once, twice or thrice (for multiple administrations, one week elapsed between treatments). One week following final administration, mice were sacrificed by CO_2 asphyxiation, blood was collected by cardiac puncture, serum was isolated, and sera from triplicate mice were pooled, heat inactivated and stored at -20°C.

$5x10^3$ ZR-75-1 were seeded in triplicate wells of 96 well plates and allowed to adhere overnight. Cells were starved in Opti-MEM for 2 h prior to transfection. RALA/pEGFP-N1 nanoparticles were prepared and incubated for 30 min in Opti-MEM containing sera (0, 0.1, 1 and 10% serum) from mice that had received the indicated treatment. Transfections were for 6 h, following which, Opti-MEM was replaced with RPMI-1640. 48 h later, cells were analyzed for EGFP expression by fluorescence microscopy using a Nikon Eclipse TE300 fluorescence microscope, and by flow cytometry using a BD FACSCalibur.

Neutralising Antibody Assay

Sera neutralizing antibody content was analyzed by ELISA.[52] Maxisorp ELISA plates (Nunc) were coated overnight at 4°C with RALA/pEGFP-N1 nanoparticles in PBS. Wells were washed with PBS/0.05% Tween 20, and blocked with PBS/1% bovine serum albumin for 1 h at room temperature. The wells were probed (1 h, room temperature) with diluted sera (1:10, 1:100, 1:1000) from mice that had received PBS, pEGFP-N1, RALA, or RALA/pEGFP-N1 nanoparticles, washed thrice with PBS/0.05% Tween 20,

and probed with an anti-mouse IgA,M,G-HRP secondary antibody (AdB Serotec). Following three further washes, tetramethylbenzidine substrate was added, quenched with 1N HCl, and absorbance quantified at 450 nm, with background absorbance (550 nm) subtracted.

iNOS transgene expression

MDA-MB-231-luc-D3H1 were plated (10^4 cells per well of a 24 well plate) and allowed to adhere overnight, and were transfected with RALA/CMV-iNOS or RALA/hOC-iNOS for 6 h, following which Opti-MEM was replaced with phenol red-free MEM/10% fetal bovine serum. 48 h later, MEM nitrite content was assayed using Greiss test for nitrites (Active Motif, Belgium) as instructed by the manufacturer. The cellular iNOS transgene expression was measured via western blot as previously described.[53]

iNOS-mediated docetaxel sensitization

MDA-MB-231-luc-D3H1 were plated in 24 well plates at 10^5 cells per well and allowed to attach overnight. Cells were transfected with RALA/hOC-iNOS or RALA/CMV-iNOS nanoparticles (0.5 μg DNA/ well) for 6 h, following which, cells were returned to DMEM. 24 h following transfection, DMEM was replaced with DMEM containing docetaxel (0, 4, 20, 100, 500, 2500 ng/ml). Following a further 48 h incubation, docetaxel-containing DMEM was replaced with DMEM containing D-luciferin (Perkin Elmer) at 150 μg/mL; subsequent to a 2 min incubation, luminescence was determined using IVIS imaging. Luminescence in wells was quantified using Living Image software (Perkin Elmer).

Establishment of metastatic disease

All animal experiments were carried out in accordance with the Animal (Scientific Procedures) Act 1986 and conformed to the current UKCCCR guidelines. Mice were bred in-house and maintained using the highest possible standard of care, and priority was given to their welfare.

Mice (6-8 weeks old) were anesthetized using isoflurane (3% in O_2) and restrained using surgical adhesive tape in a supine position. Thoracic fur was removed. Using a 1 ml syringe fitted with a 26G needle, mice were implanted with 100 µl of MDA-MB-231-luc-D3H1 at 10^6 cells/ml via the left cardiac ventricle – the cell suspension was gently injected into the ventricle, following which the needle was held in place for 10 s to minimize leakage of delivered cells from the ventricle. To confirm appropriate delivery, mice were injected with 150 mg/kg D-luciferin i.p., and after 15 min incubation, isoflurane-anesthetized mice were imaged using an IVIS200 (Xenogen) imaging system. Appropriate left ventricular delivery was indicated by appearance of luminescence throughout the mouse, while inappropriate delivery was indicated by luminescence being limited to the thoracic cavity; such mice were sacrificed by CO_2 asphyxiation.

Gene therapy regimen

Beginning 48 h post-implantation, mice received treatments twice weekly for five treatments. Treatments comprised RALA/CMV-iNOS or RALA/hOC-iNOS complexes (corresponding to 5x10 µg DNA per mouse) at N:P10, while vehicle control (RALA

equivalent to the mass of RALA used in the gene therapy regimens) and untreated controls were also performed. Treatment was via tail vein injection. A subgroup of mice received docetaxel treatment in addition to iNOS gene therapy; docetaxel treatment (5 mg/kg i.p.) commenced seven days post-implantation, and was weekly for three weeks; gene therapy treatments were as before.

Mice were monitored for micrometastases development using routine (twice weekly) IVIS imaging as described above, as well as body mass measurement. A loss of 20% original body mass was deemed sufficient to necessitate sacrifice of the mouse. The degree of whole body luminescence in mice was determined using Living Image software (Perkin Elmer). At regular intervals, blood samples were taken from mice following tail prick, and stored in EDTA-coated tubes. Blood nitrite levels were assayed using ArrowSTRAIGHT™ Nitric Oxide Measurement System (Lazar Labs).

Statistics

All statistics were performed using GraphPad Prism, version 6.0g for Mac OS X. The various tests used are described throughout.

Author contributions

Conceptualization, NJD, VLK, TR and HOM; Methodology, CMM, JWM, JM, AAA and JAC; Investigation, CMM, JWM, JM, AAA and JAC; Writing – Original Draft, CMM and HOM; Writing – Review & Editing, CMM and HOM; Funding Acquisition, VLK, TR and HOM.; Resources, VLK, TR and HOM.; Supervision, VLK, TR and HOM.

Acknowledgements

The authors wish to acknowledge the efforts of QUB's Biological Services Unit for mouse husbandry and advice. This work was supported by grants from Cancer Research UK (C17372/A14271 and C17372/A18475). The funders did not aid in experimental design, or in manuscript drafting.

References

1. McCarthy HO, McCaffrey J, McCrudden CM, Zholobenko A, Ali AA, McBride JW, et al. Development and characterization of self-assembling nanoparticles using a bio-inspired amphipathic peptide for gene delivery. J Control Release 2014 Sep 10;189:141-149.

2. Bennett R, Yakkundi A, McKeen HD, McClements L, McKeogh TJ, McCrudden CM, et al. RALA-mediated delivery of FKBPL nucleic acid therapeutics. Nanomedicine (Lond) 2015 Sep 30.

3. Massey AS, Pentlavalli S, Cunningham R, McCrudden CM, McErlean EM, Redpath P, et al. Potentiating the Anticancer Properties of Bisphosphonates by Nanocomplexation with the Cationic Amphipathic Peptide, RALA. Mol Pharm 2016 Apr 4;13(4):1217-1228.

4. Huerta S, Chilka S, Bonavida B. Nitric oxide donors: novel cancer therapeutics (review). Int J Oncol 2008 Nov;33(5):909-927.

5. Singh S, Gupta AK. Nitric oxide: role in tumour biology and iNOS/NO-based anticancer therapies. Cancer Chemother Pharmacol 2011 Jun;67(6):1211-1224.

6. Cui S, Reichner JS, Mateo RB, Albina JE. Activated murine macrophages induce apoptosis in tumor cells through nitric oxide-dependent or -independent mechanisms. Cancer Res 1994 May 1;54(9):2462-2467.

7. McMurtry V, Saavedra JE, Nieves-Alicea R, Simeone AM, Keefer LK, Tari AM. JS-K, a nitric oxide-releasing prodrug, induces breast cancer cell death while sparing normal mammary epithelial cells. Int J Oncol 2011 Apr;38(4):963-971.

8. Miller MR, Megson IL. Recent developments in nitric oxide donor drugs. Br J Pharmacol 2007 Jun;151(3):305-321.

9. Adams C, McCarthy HO, Coulter JA, Worthington J, Murphy C, Robson T, et al. Nitric oxide synthase gene therapy enhances the toxicity of cisplatin in cancer cells. J Gene Med 2009 Feb;11(2):160-168.

10. Coulter JA, McCarthy HO, Worthington J, Robson T, Scott S, Hirst DG. The radiation-inducible pE9 promoter driving inducible nitric oxide synthase radiosensitizes hypoxic tumour cells to radiation. Gene Ther 2008 Apr;15(7):495-503.

11. Coulter JA, Page NL, Worthington J, Robson T, Hirst DG, McCarthy HO. Transcriptional regulation of inducible nitric oxide synthase gene therapy: targeting early stage and advanced prostate cancer. J Gene Med 2010 Sep;12(9):755-765.

12. McCarthy HO, Worthington J, Barrett E, Cosimo E, Boyd M, Mairs RJ, et al. p21((WAF1))-mediated transcriptional targeting of inducible nitric oxide synthase gene therapy sensitizes tumours to fractionated radiotherapy. Gene Ther 2007 Feb;14(3):246-255.

13. McCarthy HO, Zholobenko AV, Wang Y, Canine B, Robson T, Hirst DG, et al. Evaluation of a multi-functional nanocarrier for targeted breast cancer iNOS gene therapy. Int J Pharm 2011 Feb 28;405(1-2):196-202.

14. Worthington J, McCarthy HO, Barrett E, Adams C, Robson T, Hirst DG. Use of the radiation-inducible WAF1 promoter to drive iNOS gene therapy as a novel anti-cancer treatment. J Gene Med 2004 Jun;6(6):673-680.

15. Chen YF, Jiang XZ, He LY, Tang YX, Long Z. Transfection of iNOS suppresses the growth of androgen-independent prostate cancer DU145 cells. Zhonghua Nan Ke Xue 2012 Aug;18(8):697-702.

16. Tan J, Zeng Q, Jiang XZ, He LY, Wang JR, Yao K, et al. Apoptosis of bladder transitional cell carcinoma T24 cells induced by adenovirus-mediated inducible nitric oxide synthase gene transfection. Chin J Cancer Res 2013 Oct;25(5):593-599.

17. Ye S, Yang W, Wang Y, Ou W, Ma Q, Yu C, et al. Cationic liposome-mediated nitric oxide synthase gene therapy enhances the antitumor effects of cisplatin in lung cancer. Int J Mol Med 2013 Jan;31(1):33-42.

18. Yeung F, Law WK, Yeh CH, Westendorf JJ, Zhang Y, Wang R, et al. Regulation of human osteocalcin promoter in hormone-independent human prostate cancer cells. J Biol Chem 2002 Jan 25;277(4):2468-2476.

19. McCarthy HO, Coulter JA, Worthington J, Robson T, Hirst DG. Human osteocalcin: a strong promoter for nitric oxide synthase gene therapy, with specificity for hormone refractory prostate cancer. J Gene Med 2007 Jun;9(6):511-520.

20. Ali AA, Coulter JA, Ogle CH, Migaud MM, Hirst DG, Robson T, et al. The contribution of N2O3 to the cytotoxicity of the nitric donor drug DETA/NO; an emerging role for S-nitrosylation. Biosci Rep 2013 Feb 13.

21. McCaffrey J, McCrudden CM, Ali AA, Massey AS, McBride JW, McCrudden MTC, et al. Transcending epithelial and intracellular biological barriers; a prototype DNA delivery device. J Controlled Release 2016 3/28;226:238-247.

22. Heinecke JL, Ridnour LA, Cheng RY, Switzer CH, Lizardo MM, Khanna C, et al. Tumor microenvironment-based feed-forward regulation of NOS2 in breast cancer progression. Proc Natl Acad Sci U S A 2014 Apr 29;111(17):6323-6328.

23. Diez S, Navarro G, de ILarduya CT. In vivo targeted gene delivery by cationic nanoparticles for treatment of hepatocellular carcinoma. J Gene Med 2009 Jan;11(1):38-45.

24. Xu W, Liu L, Charles IG. Microencapsulated iNOS-expressing cells cause tumor suppression in mice. FASEB J 2002 Feb;16(2):213-215.

25. Bonavida B, Khineche S, Huerta-Yepez S, Garban H. Therapeutic potential of nitric oxide in cancer. Drug Resist Updat 2006 Jun;9(3):157-173.

26. Xie K, Huang S, Dong Z, Juang SH, Wang Y, Fidler IJ. Destruction of bystander cells by tumor cells transfected with inducible nitric oxide (NO) synthase gene. J Natl Cancer Inst 1997 Mar 19;89(6):421-427.

27. Holland RJ, Paulisch R, Cao Z, Keefer LK, Saavedra JE, Donzelli S. Enzymatic generation of the NO/HNO-releasing IPA/NO anion at controlled rates in physiological media using beta-galactosidase. Nitric Oxide 2013 Nov 30;35:131-136.

28. Sharma K, Sengupta K, Chakrapani H. Nitroreductase-activated nitric oxide (NO) prodrugs. Bioorg Med Chem Lett 2013 Nov 1;23(21):5964-5967.

29. Ning S, Bednarski M, Oronsky B, Scicinski J, Saul G, Knox SJ. Dinitroazetidines are a novel class of anticancer agents and hypoxia-activated radiation sensitizers developed from highly energetic materials. Cancer Res 2012 May 15;72(10):2600-2608.

30. Kim J, Wilson DR, Zamboni CG, Green JJ. Targeted polymeric nanoparticles for cancer gene therapy. J Drug Target 2015;23(7-8):627-641.

31. Taipaleenmaki H, Browne G, Akech J, Zustin J, van Wijnen AJ, Stein JL, et al. Targeting of Runx2 by miR-135 and miR-203 Impairs Progression of Breast Cancer and Metastatic Bone Disease. Cancer Res 2015 Apr 1;75(7):1433-1444.

32. Ge C, Zhao G, Li Y, Li H, Zhao X, Pannone G, et al. Role of Runx2 phosphorylation in prostate cancer and association with metastatic disease. Oncogene 2016 Jan 21;35(3):366-376.

33. Robson T, Hirst DG. Transcriptional Targeting in Cancer Gene Therapy. J Biomed Biotechnol 2003;2003(2):110-137.

34. Baniwal SK, Khalid O, Gabet Y, Shah RR, Purcell DJ, Mav D, et al. Runx2 transcriptome of prostate cancer cells: insights into invasiveness and bone metastasis. Mol Cancer 2010 Sep 23;9:258-4598-9-258.

35. Hsu YL, Huang MS, Yang CJ, Hung JY, Wu LY, Kuo PL. Lung tumor-associated osteoblast-derived bone morphogenetic protein-2 increased epithelial-to-mesenchymal transition of cancer by Runx2/Snail signaling pathway. J Biol Chem 2011 Oct 28;286(43):37335-37346.

36. Niu DF, Kondo T, Nakazawa T, Oishi N, Kawasaki T, Mochizuki K, et al. Transcription factor Runx2 is a regulator of epithelial-mesenchymal transition and invasion in thyroid carcinomas. Lab Invest 2012 Aug;92(8):1181-1190.

37. Juang SH, Xie K, Xu L, Shi Q, Wang Y, Yoneda J, et al. Suppression of tumorigenicity and metastasis of human renal carcinoma cells by infection with retroviral vectors harboring the murine inducible nitric oxide synthase gene. Hum Gene Ther 1998 Apr 10;9(6):845-854.

38. Wang Z, Cook T, Alber S, Liu K, Kovesdi I, Watkins SK, et al. Adenoviral gene transfer of the human inducible nitric oxide synthase gene enhances the radiation response of human colorectal cancer associated with alterations in tumor vascularity. Cancer Res 2004 Feb 15;64(4):1386-1395.

39. Tschugguel W, Schneeberger C, Unfried G, Czerwenka K, Weninger W, Mildner M, et al. Expression of inducible nitric oxide synthase in human breast cancer depends on tumor grade. Breast Cancer Res Treat 1999 Jul;56(2):145-151.

40. Cheng RYS, Basudhar D, Ridnour LA, Heinecke JL, Kesarwala AH, Glynn S, et al. Gene expression profiles of NO- and HNO-donor treated breast cancer cells: insights into tumor response and resistance pathways. Nitric Oxide 2014 12/1;43(0):17-28.

41. Glynn SA, Boersma BJ, Dorsey TH, Yi M, Yfantis HG, Ridnour LA, et al. Increased NOS2 predicts poor survival in estrogen receptor-negative breast cancer patients. J Clin Invest 2010 Nov;120(11):3843-3854.

42. Granados-Principal S, Liu Y, Guevara ML, Blanco E, Choi DS, Qian W, et al. Inhibition of iNOS as a novel effective targeted therapy against triple negative breast cancer. Breast Cancer Res 2015 Dec;17(1):527-015-0527-x. Epub 2015 Feb 22.

43. Luke JJ, LoRusso P, Shapiro GI, Krivoshik A, Schuster R, Yamazaki T, et al. ASP9853, an inhibitor of inducible nitric oxide synthase dimerization, in combination with docetaxel: preclinical investigation and a Phase I study in advanced solid tumors. Cancer Chemother Pharmacol 2016 Mar;77(3):549-558.

44. Perske C, Lahat N, Sheffy Levin S, Bitterman H, Hemmerlein B, Rahat MA. Loss of inducible nitric oxide synthase expression in the mouse renal cell carcinoma cell line RENCA is mediated by microRNA miR-146a. Am J Pathol 2010 Oct;177(4):2046-2054.

45. Fkih M'hamed I, Privat M, Ponelle F, Penault-Llorca F, Kenani A, Bignon YJ. Identification of miR-10b, miR-26a, miR-146a and miR-153 as potential triple-negative breast cancer biomarkers. Cell Oncol (Dordr) 2015 Dec;38(6):433-442.

46. Rabender CS, Alam A, Sundaresan G, Cardnell RJ, Yakovlev VA, Mukhopadhyay ND, et al. The Role of Nitric Oxide Synthase Uncoupling in Tumor Progression. Mol Cancer Res 2015 Feb 27.

47. Hernandez-Vargas H, Palacios J, Moreno-Bueno G. Molecular profiling of docetaxel cytotoxicity in breast cancer cells: uncoupling of aberrant mitosis and apoptosis. Oncogene 2007 May 3;26(20):2902-2913.

48. Pervin S, Singh R, Chaudhuri G. Nitric oxide-induced cytostasis and cell cycle arrest of a human breast cancer cell line (MDA-MB-231): potential role of cyclin D1. Proc Natl Acad Sci U S A 2001 Mar 13;98(6):3583-3588.

49. Matthews NE, Adams MA, Maxwell LR, Gofton TE, Graham CH. Nitric oxide-mediated regulation of chemosensitivity in cancer cells. J Natl Cancer Inst 2001 Dec 19;93(24):1879-1885.

50. Ansari S, Madhu B, Robinson SP, Whitley GSJ. Docetaxel effect on tumorigenic C6 glioma cells is nitric oxide dependent. Cancer Epidemiology Biomarkers & Prevention 2006 December 01;15(12 Supplement):B122-B122.

51. Yasuda H, Nakayama K, Watanabe M, Suzuki S, Fuji H, Okinaga S, et al. Nitroglycerin treatment may enhance chemosensitivity to docetaxel and carboplatin in patients with lung adenocarcinoma. Clin Cancer Res 2006 Nov 15;12(22):6748-6757.

52. Barker SE, Broderick CA, Robbie SJ, Duran Y, Natkunarajah M, Buch P, et al. Subretinal delivery of adeno-associated virus serotype 2 results in minimal immune responses that allow repeat vector administration in immunocompetent mice. J Gene Med 2009 Jun;11(6):486-497.

53. Coulter JA, Page NL, Worthington J, Robson T, Hirst DG, McCarthy HO. Transcriptional regulation of inducible nitric oxide synthase gene therapy: targeting early stage and advanced prostate cancer. J Gene Med 2010 Sep;12(9):755-765.

List of abbreviations

(i)NOS – (inducible) nitric oxide synthase; CMV – cytomegalovirus; hOC - human osteocalcin; ·NO – nitric oxide; PSMA - prostate specific membrane antigen; EGFP – enhanced green fluorescent protein; N:P – Nitrogen:phosphate; FITC – fluorescein isothiocyanate; DAPI - 4',6-diamidino-2-phenylindole; ELISA - enzyme-linked immunosorbent assay; HCl – hydrochloric acid; UKCCCR - United Kingdom Co-ordinating Committee on Cancer Research; IVIS – in vivo imaging system; ANOVA – Analysis of variance

Conflict of interest statement

The authors declare that they have no conflicting interests.

Figure legends

Figure 1 - Complexation of plasmid DNA with RALA produces nanoparticles suitable for cellular delivery.

A, incubation of plasmid DNA with RALA resulted in nanoparticles that did not exceed 100 nm in diameter, with a positive charge of approximately 20-25 mV. *B*, Cy3-labeled DNA forms nanoparticles with RALA that resemble those formed with unlabeled DNA. Datapoints represent mean ± SD; N ≥ 3. *C*, orthogonal sectioning of Z-stacks of MDA-MB-231-luc-D3H1 transfected with RALA/Cy3-pEGFP-1. RALA is delivers plasmid DNA to the nucleus of MDA-MB-231-luc-D3H1 within 120 min. Green – actin cytoskeleton; blue – nucleus; red – Cy3.

Figure 2 - Administration of RALA/pEGFP-N1 nanoparticles to immunocompetent mice does not provoke a neutralizing antibody response.

A, flow cytometric analysis of GFP in ZR-75-1 after incubation of RALA/pEGFP-N1 nanoparticles with sera from C57BL/6 mice that received the indicated treatment (PBS/DNA/RALA/NPs) weekly for up to 3 weeks. *p<0.05, **p<0.01, ***p<0.001 compared to expression elicited by RALA/pEGFP-N1 nanoparticles (NP) that had been incubated in sera from mice that had received nanoparticles (multiple comparisons ANOVA). *B*, fluorescence micrographs of ZR-75-1 transfected with RALA/pEGFP-N1 nanoparticles following incubation in FBS or serum from mice that received two administrations of RALA/pEGFP-N1. *C*, sera neutralizing antibody (immunoreactivity of an anti-mouse IgA, IgG and IgM) content analyzed by ELISA. Datapoints represent mean ± SD; N ≥ 3.

Figure 3- Validation of hOC- and CMV-driven iNOS plasmids.

A, iNOS protein expression in MDA-MB-231-luc-D3H1 48 h post-transfection with RALA/hOC-iNOS or RALA/CMV-iNOS (comprising 0.5 μg DNA) at N:P10 for 6 h; ·NO generation was confirmed by Greiss test. *B*, MDA-MB-231-luc-D3H1 overexpressing iNOS form fewer clonogenic colonies, which is partially inhibited by 1 mM aminoguanidine. Datapoints represent mean ± SD; N = 3.

Figure 4 - Treatment with RALA/hOC-iNOS or RALA/CMV-iNOS improves survival of MDA-MB-231-luc-D3H1 metastases-bearing mice.

A, IVIS images of mice (control and RALA/iNOS) at indicated timepoints post-implantation. *B*, survival of metastases-bearing mice (N=6 (control, RALA) or ≥ 9 (either RALA/iNOS strategy)). *C*, weight loss of exemplar mice. *D*, total bioluminescence in exemplar mice; inverted triangles denote treatment timepoints. *E*, relative blood nitrite levels in control, RALA/hOC-iNOS and RALA/CMV-iNOS treated mice.

Figure 5 - Assessment of iNOS overexpression on sensitization of MDA-MB-231-luc-D3H1 to docetaxel.

A, transfection of MDA-MB-231-luc-D3H1 with RALA/hOC-iNOS or RALA/CMV-iNOS increases the potency of docetaxel *in vitro*. *B*, RALA/hOC-iNOS or RALA/CMV-iNOS treatment produces a slight additive improvement in response to docetaxel in MDA-MB-231-luc-D3H1 metastases-bearing mice. N≥5. *C* and *D*, weight loss and

bioluminescence accumulation data for exemplar mice; closed inverted triangles denote gene therapy treatment, open inverted triangles denote docetaxel treatment.

Figure 1

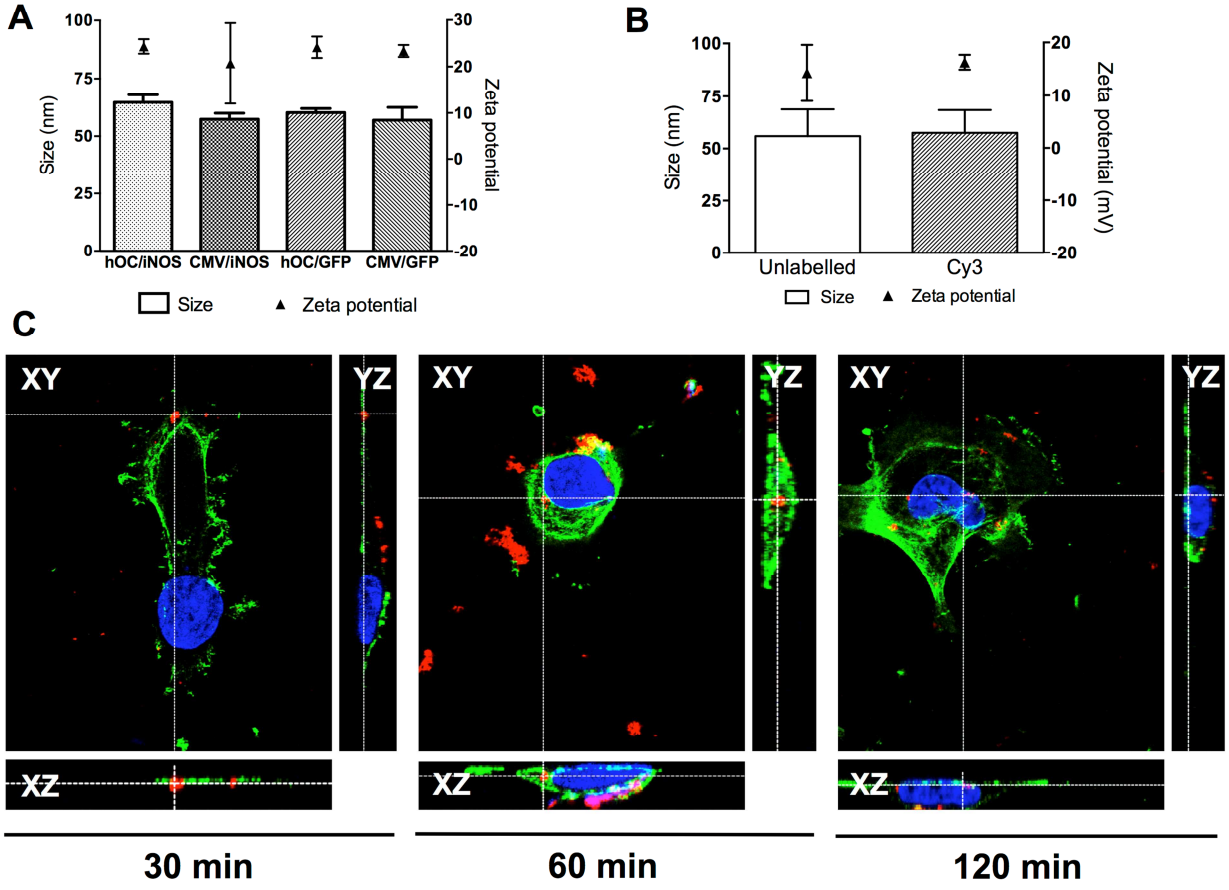

Figure 2

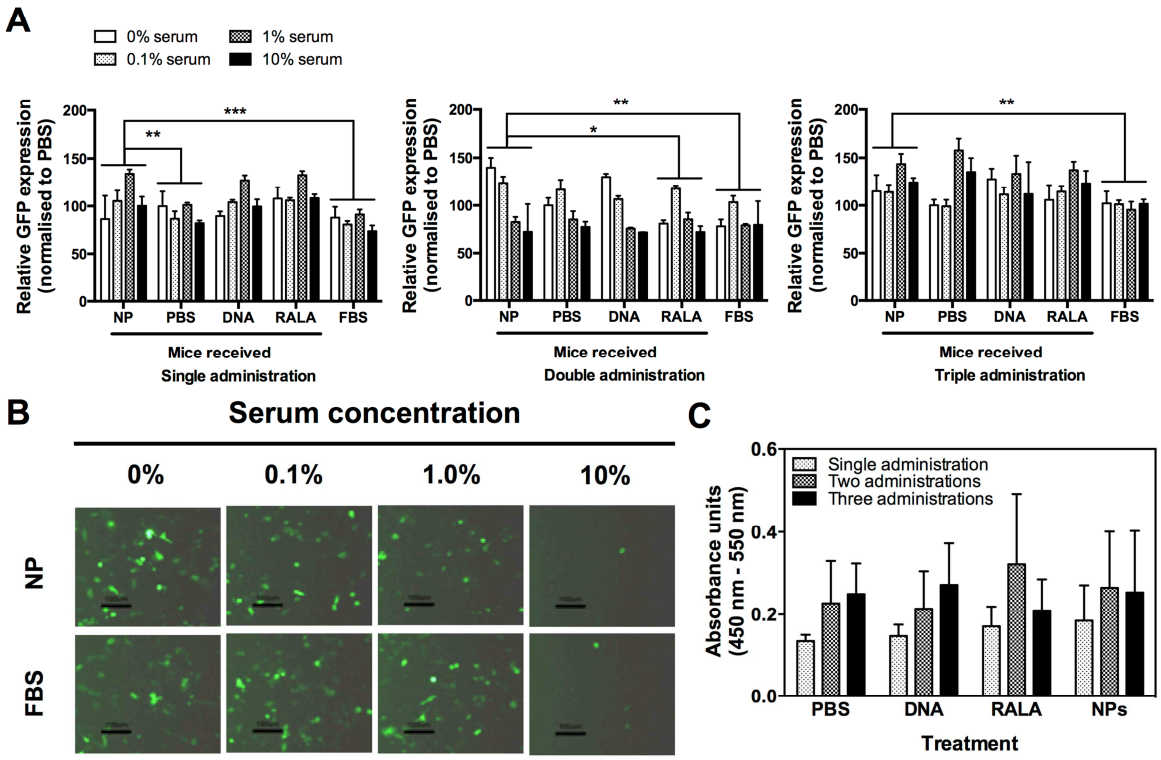

Figure 3

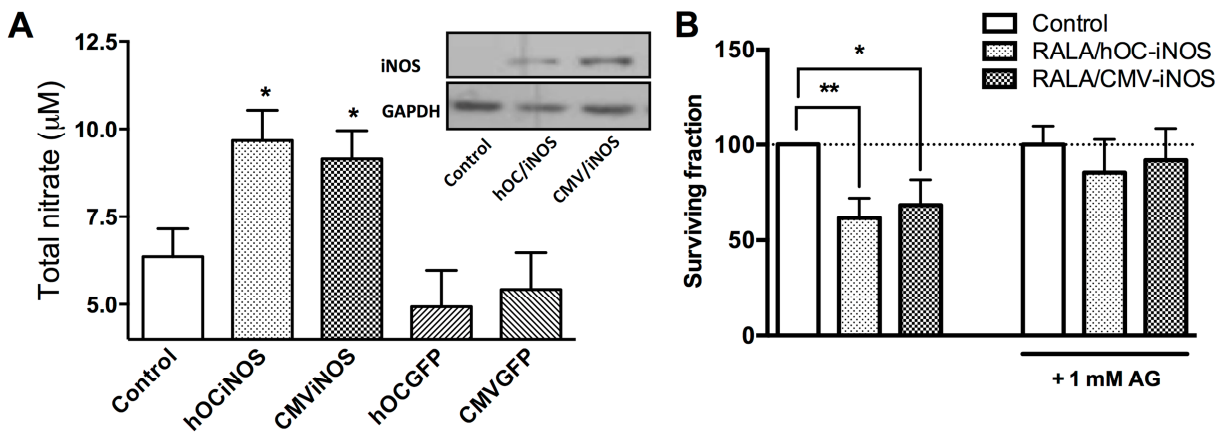

Figure 4

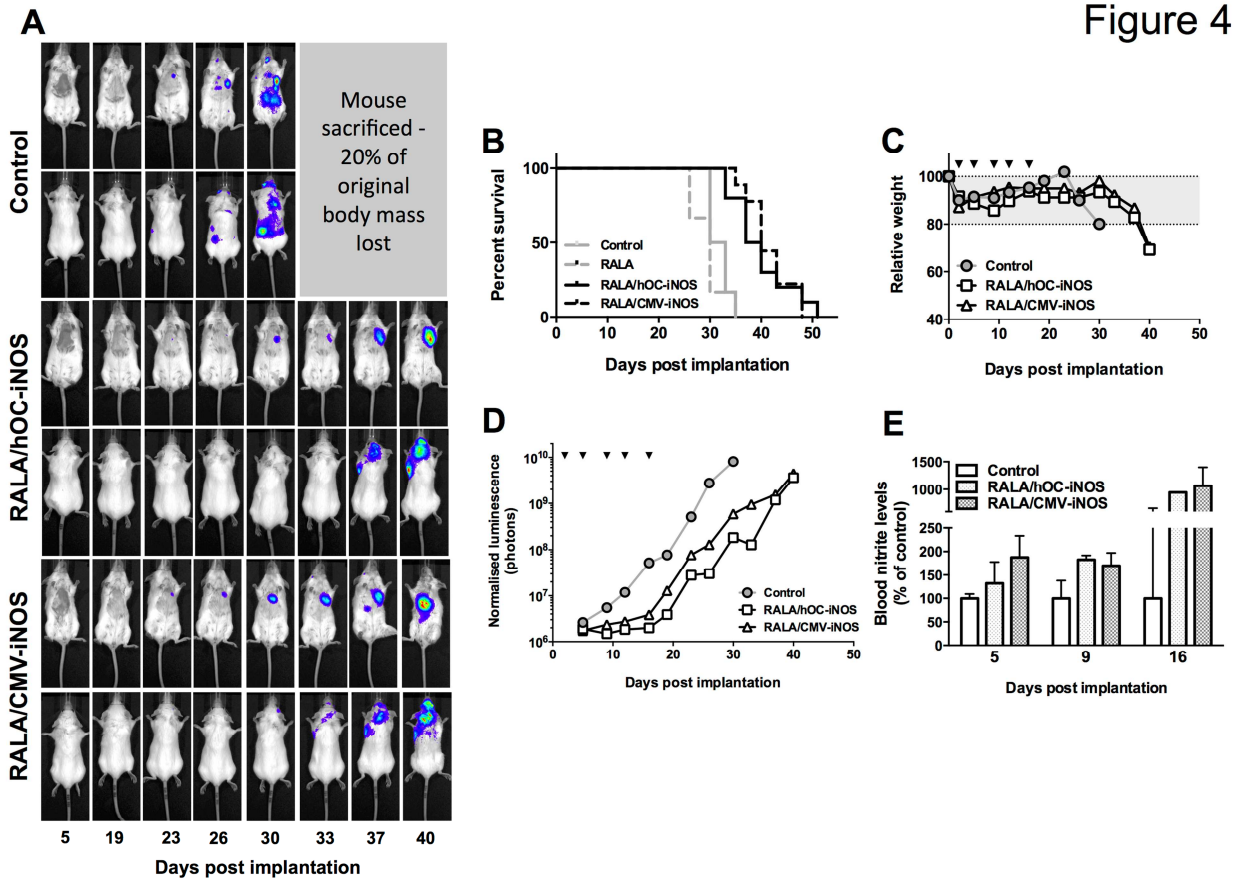

Figure 5